Electronic Supplementary Material (ESI) for Nanoscale.
This journal is © The Royal Society of Chemistry 2022

Melamine-Graphene Epoxy Nanocomposite Based Die Attach Films for Advanced 3D Semiconductor Packaging Applications

Zhijian Sun[a], Ryan Wong[a], Yifan Liu[a], Michael Yu[a], Jiaxiong Li[a], Daron Spence[a], Mingyue Zhang[a], Mohanalingam Kathaperumal[b], Ching-Ping Wong[a*]

[a] School of Materials Science and Engineering, Georgia Institute of Technology, Atlanta, Georgia 30332, United States.

[b] School of Electrical and Computing Engineering, Georgia Institute of Technology, Atlanta, Georgia 30332, United States.

Corresponding author: cp.wong@mse.gatech.edu (C.P. Wong)

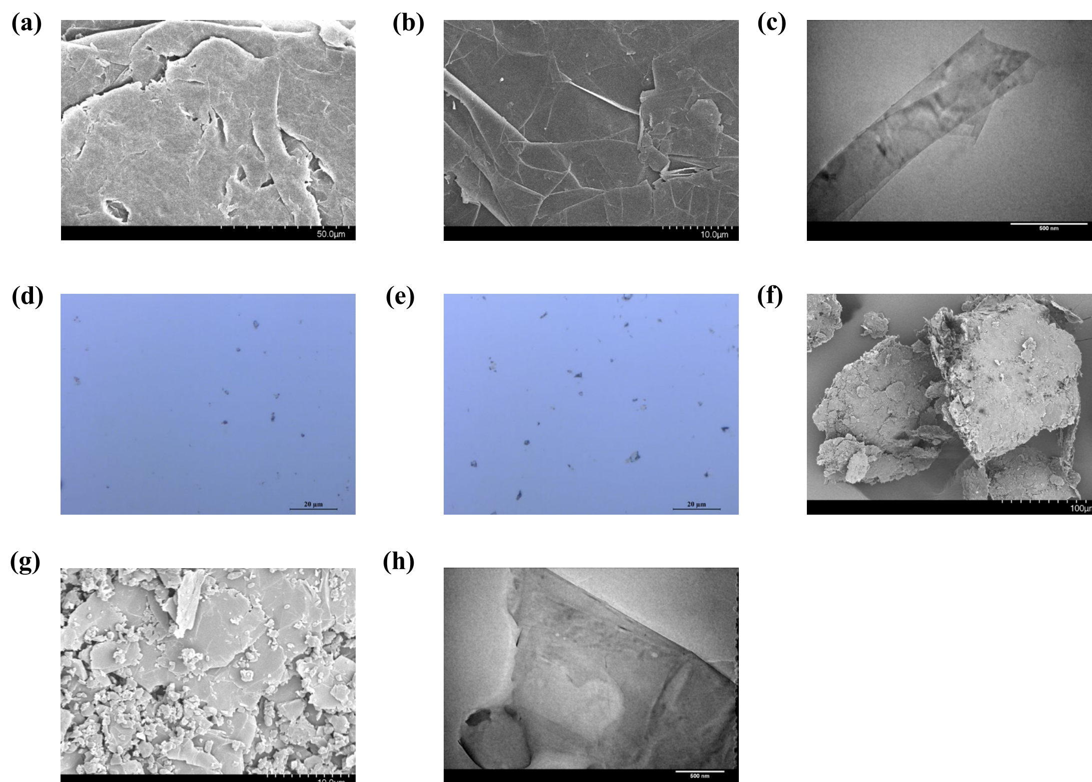

Figure S1. (a, b) SEM images of graphene nanosheets at different magnifications. (c) TEM image of graphene nanosheets. OM images of (d) graphene nanosheets and (e) M-G at ×100 magnification. (f, g) SEM images of M-G at different magnifications. (h) TEM image of M-G.

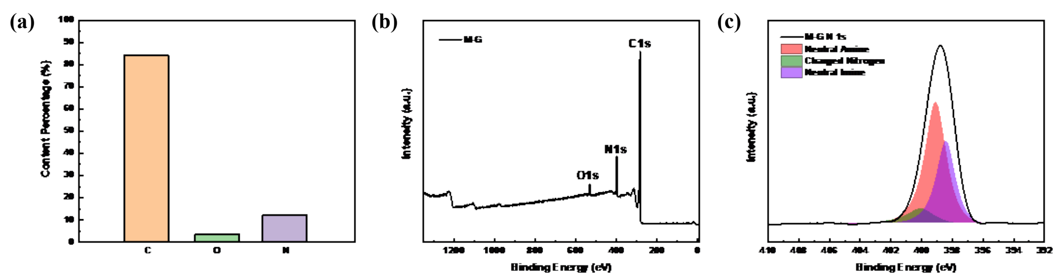

Figure S2. (a) Element content percentage of M-G. (b) XPS survey of M-G. (c) XPS spectra of M-G in N 1s.

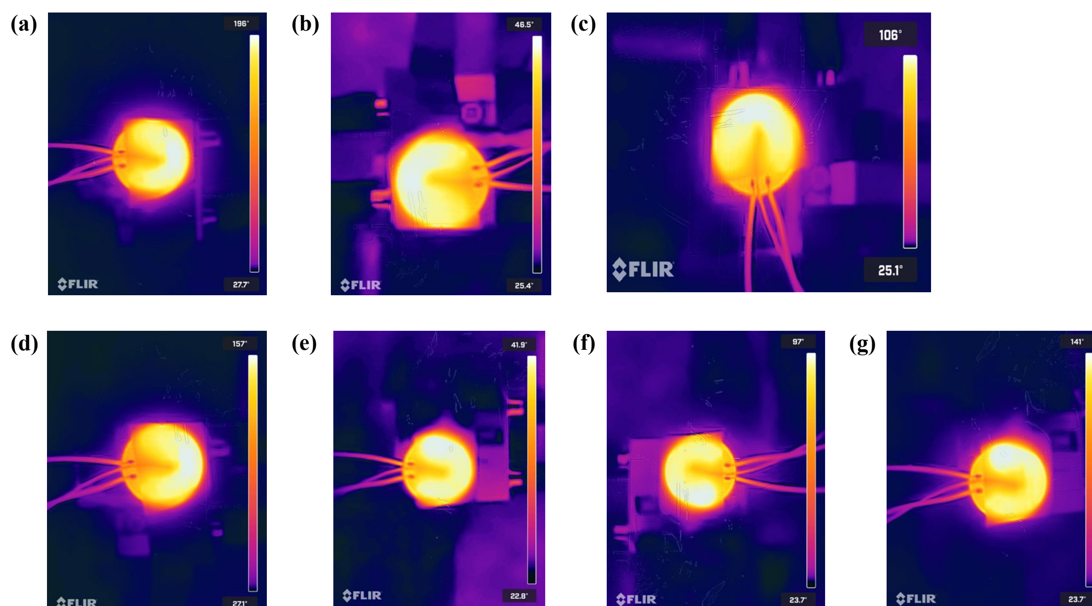

Figure S3. IR image of ceramic heater for neat epoxy as DAFs at power of (a) 15 W, (b) 10W, (c) 5W and (d) 1W. IR image of ceramic heater for M-G epoxy nanocomposites as DAFs at power of (e) 10 W, (f) 5W and (g) 1W.

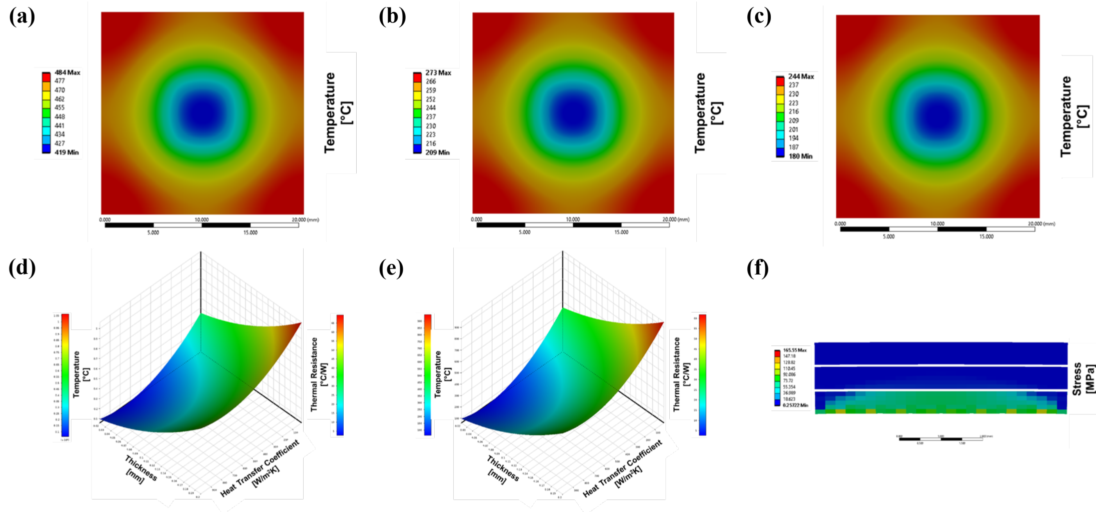

Figure S4. The modeling ceramic heater temperature of (a) neat epoxy, (b) 1 wt% graphene epoxy nanocomposites and (c) 1 wt% M-G epoxy nanocomposites as DAFs at power of 15W. The response 3D surfaces images of (d) 1 wt% graphene epoxy nanocomposites and (e) 1 wt% M-G epoxy nanocomposites between the different parameters. (f) The modeling thermal stress of three dies in configuration system for 1 wt% M-G epoxy nanocomposites as DAFs.

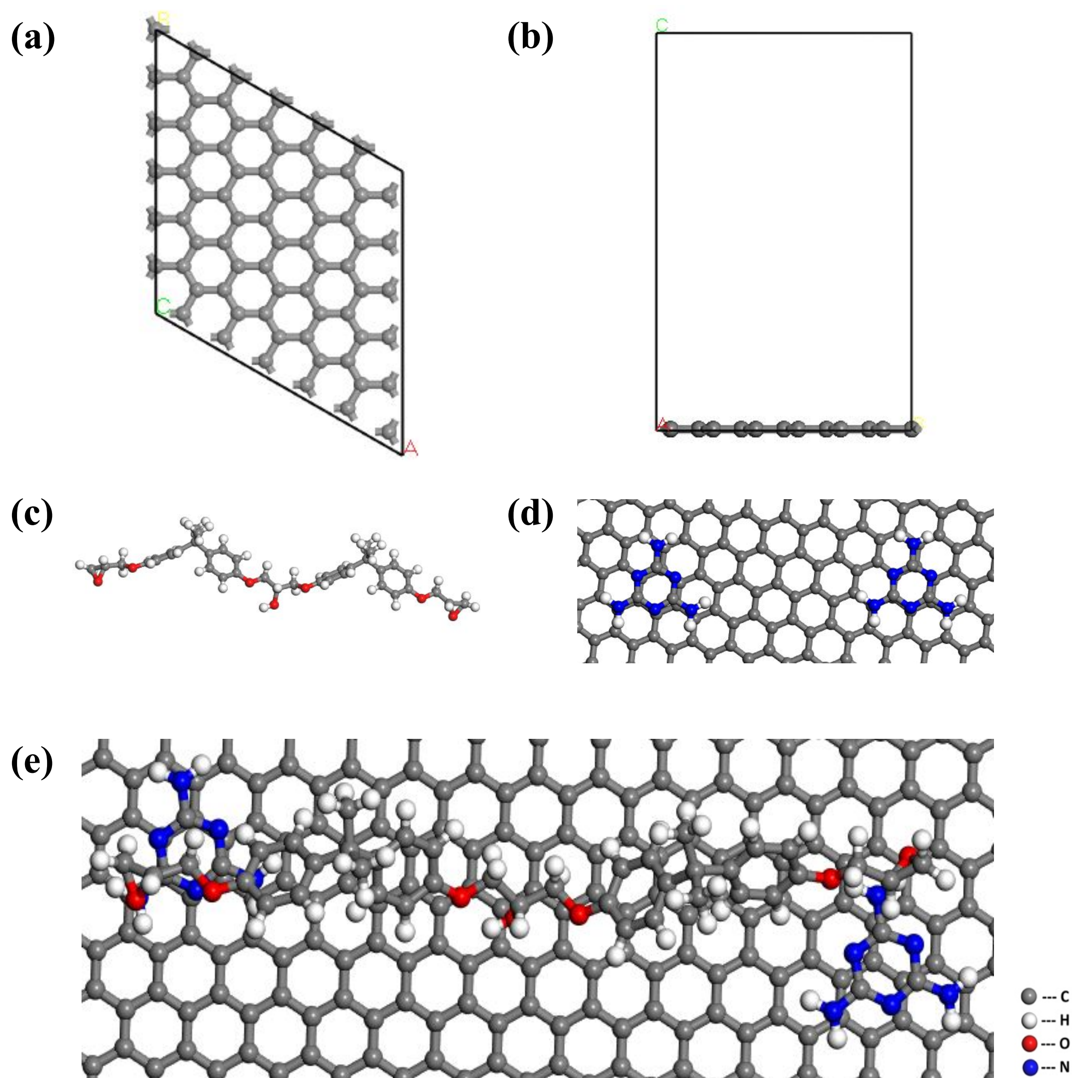

Figure S5. The graphene unit cell of (a) top view and (b) cross view consisting of 72 carbon atoms with a 20 Å vacuum perpendicular to the graphene surface. (c) The structure of neat epoxy resins. (d) The top view of the M-G structure for the epoxy adsorption study. (e) The top view of the M-G-epoxy relaxed configuration.

Table S1. Thermal conductivity of silver-epoxy nanocomposites with different loadings.

Silver-Epoxy Nanocomposite Sample Filler	**Thermal Conductivity (W/mk)**	**Loading**	**Ref.**
Sintered Ag NPs/BNNS	1.13	20 wt%	[1]
Ag-deposited BNNS	3.06	25.1 vol%	[2]
Ag NPs/modified BNNS	2.14	25 vol%	[3]
Ag NPs/MXene nanosheets	2.65	15.1 vol%	[4]
MWCNT-Fe_3O_4@Ag	0.46	15 wt%	[5]
MWCNT-polypyrrole Ag NPs	0.47	10 wt%	[6]
Alumina/polydopamine@Ag	0.60	22.9 vol%	[7]
Ag NWs	1.25	9.54 wt%	[8]
Ag NWs@SiO_2	1.030	4 vol%	[9]
Ag NPs/Ag NWs/BNNS	0.804	-	[10]
Ag NWs/functionalized graphene	1.413	4 vol%	[11]

Experimental Section

Materials:

Graphene nanosheets were purchased from ACS Material. Melamine was purchased from Alfa Aesar. N,N-Dimethylformamide (DMF) was purchased from VWR. Epoxy resin 828 (Bisphenol A diglycidyl ether) was obtained from Hexion, and cresol novolac epoxy was obtained from Sumitomo Chemical. The HMPA (hexahydro-4-methylphthalic anhydride) hardener was obtained from Lindau chemicals, Inc, and the catalysts,1-cyanoethyl-2-ethyl-4-methylimidazoles which were purchased from Sigma-Aldrich.

Preparation of melamine functionalized graphene epoxy nanocomposites:

The melamine functionalized graphene nanosheets were synthesized by the following method. 0.5 g Melamine was dissolved in 80 mL DMF by stirring and sonication. Then 0.5 g graphene nanosheets was added to the above solution by stirring and sonication until the graphene dispersed uniformly in the solution. The resulting mixture was transferred into 4 oz. polypropylene jars and subjected to ball-milling for 24 hrs at 200 rpm. Two different sizes of zirconia balls were used in each jar: 50 small 3-mm diameter balls and 20 large 5-mm diameter balls. The mass ratio of material to balls is 1: 10. The powders were collected by vacuum filtration, using ethanol during vacuum filtration to wash them before collection. They were then dried at room temperature in a vacuum oven for 24 hrs.

Epoxy nanocomposites were made by mixing cresol novolac epoxy with bisA epoxy in the acetone solution, and then added filler into solution. The dispersing functionalized

graphene nanosheets in epoxy resin (epoxy: curing agent: catalyst = 1: 0.8: 0.01) at different loading levels under stirring and sonication until homogeneous samples were obtained. Before curing process, the samples will be put into the vacuum oven at 60 ℃ to remove the acetone. Then the samples were transferred to aluminum pans and cured at 155 °C for 90 mins.

Characterization:

SEM images of the fillers were taken using FE-SEM (SU8230, Hitachi, Japan). TEM images of the fillers were taken on a JEOL TEM (100CX II, JEOL, Japan). AFM images of the fillers were taken by AFM (Dimension Edge, Veeco, U.S.A.). OM images of the filler were taken on an optical microscopy at 100X (Lecia DM 4000M, German). XPS characterization was carried out with K-Alpha XPS (Thermo Scientific, U.S.A.). FTIR spectra were recorded using Nicolet iS5 FTIR (Thermo Fisher Scientific, U.S.A.). The TGA tests were programmed to increase at 10 °C/min from 40 °C to 800 °C under a 100 mL/min nitrogen flow (SDT Q600, TA Instruments, U.S.A.). Raman characterization was carried out using an UV Raman Microscope with a 488 nm wavelength laser (Renishaw, United Kingdom). XRD patterns were recorded by Alpha-1(Malvern PANalytical, United Kingdom) with Cu Kα radiation (λ: 1.54 Å). DMA was performed in a tension mode with an increased rate of 3 °C/min from room temperature to 300 °C in an air atmosphere at an oscillation frequency of 1 Hz (DMA Q800, TA Instruments, U.S.A). The thermal conductivity values of epoxy composites were measured by Trident (C-THERM, Canada). It uses a single-sided, interfacial heat reflectance sensor that applies a momentary constant heat source to the sample. The

dimensions of the samples for thermal conductivity measurements are about a 1-inch diameter with a 1 mm thickness. A known current is applied to the sensor's spiral heating element, providing a small amount of heat. A guard ring surrounds the sensor coil to support a one-dimensional heat transfer into the sample. The applied current results in a rise in temperature at the interface between the sensor and the sample, which induces a change in the voltage drop of the sensor element. The rate of increase in the sensor voltage is used to determine the thermal properties of the sample. Thermal mechanical analysis (TMA) was performed at an increasing rate of 20 °C/min from 40 °C to 250 °C under a 50 mL/min nitrogen flow (TMA Q400, TA Instruments, U.S.A.) with an expansion probe. The moisture absorption measurement was performed at 85 °C/85 relative humidity (RH) atmosphere in HAST Pressure Temperature Humidity Chamber (TPC-422M, ESPEC, U.S.A). The electrical resistance was measured by electrochemical workstation (ZENNIUM, U.S.A). The sample size of these two characterizations is circle shape, which is around 1 inch diameter and 1mm thickness. The IR photos were captured by using an infrared camera (FLIR ONE Pro, U.S.A). During the performance test, the die attach films thickness were controlled by using 75 um spacers, which are SiO_2 sphere particles (diameters are 75 um). They were mixed with epoxy composites firstly before the curing process to control the thickness.

Computational methods:

The DFT simulation was conducted through Vienna Ab Initio Simulation Package (VASP),[12–14] and the ion-electron interaction was modeled using the projector-augmented wave (PAW) methodology.[15] The Perdew–Burke–Ernzerhof (PBE

exchange-correlation (XC) function was used to treat the quantum mechanical part of the electron-electron interactions.[16] Figure S5a-e illustrates the structures that we used in this study and all configurations in the simulation were fully relaxed.

Interfacial thermal resistance calculation:

For all of epoxy nanocomposites, the K_m is 0.167 W/mK for epoxy resins and the K_p are 4000 W/mK and 800 W/mK for G and M-G fillers, respectively; V_f is the volume fraction of the fillers, which was calculated from 1 wt% filler to get 0.53 vol% and 10 wt% filler to get 5.55 vol%; d is the average thickness of 50 nm and 0.3 μm for G and M-G fillers, respectively; and K is thermal conductivity for their epoxy nanocomposites.

Finite Element Model:

As the focus of this FEM study, the material stack-up was composed of three stacked dies (s = 20.92 mm, t = 0.52 mm) with layers of conformal DAF at their interfaces. For a heat-generating source, a ceramic heater (d = 23.6 mm, t = 1.25 mm) was attached at the top of the stack-up. For heat extraction, a copper heatsinks (h = 300 W/m^{2}K) was attached at the bottom of the stack-up. Due to the simple geometries of the different bodies in this stackup – heater, dies, and die attach films – hexahedron (HEX8) elements were used. There was a total of 10,366 elements and 43,790 nodes such that mesh independence was achieved. Therefore, additional mesh refinement did not affect thermomechanical simulations. Responses converged to repeatable solutions. It is important to achieve mesh convergence, especially given the differences in scale

of some of the bodies in this stackup – in comparison of heater and dies to the comparatively much thinner films. Furthermore, as geometric parameters such as thicknesses of these films were varied, all the more important to have sufficiently fine meshes to account for these changes. Different types of materials and thicknesses (t) were evaluated for the DAF layer, to assess the effectiveness of each nanocomposite as well as any critical geometric considerations for heat spreading or dissipation. Furthermore, the heat transfer coefficients (h) were also varied and evaluated, to determine the complexity of cooling solution necessary to maintain operational temperatures – such as free or forced, air or liquid. It was analyzed in steady-state conditions, as representative of the worst thermal scenarios of constant power output.

For the thermal model, the active side of the ceramic heater was implemented as a surface heat source with 15 W in losses. For the thermomechanical model, the copper heatsink was set as a fixed support, and the entire stack-up was subjected to isothermal heating as representative of passive thermal cycling, from -55°C to 150°C. For the parametric modeling study, for instance, it is demonstrated that the particular type of cooling solution has the greatest effect on temperatures and thermal resistances, in that maximum junction temperature vary more as a function of heat transfer coefficient than as a function of thickness. Other trends for minimizing temperatures include thinner DAFs for lower thermal resistances.

References

[1] C. Chen, Y. Xue, Z. Li, Y. Wen, X. Li, F. Wu, X. Li, D. Shi, Z. Xue, X. Xie,

Construction of 3D boron nitride nanosheets/silver networks in epoxy-based composites with high thermal conductivity via in-situ sintering of silver nanoparticles, Chem. Eng. J. 369 (2019) 1150–1160.

[2] F. Wang, X. Zeng, Y. Yao, R. Sun, J. Xu, C.-P. Wong, Silver Nanoparticle-Deposited Boron Nitride Nanosheets as Fillers for Polymeric Composites with High Thermal Conductivity, Sci. Rep. 6 (2016) 19394.

[3] Y. Wu, X. Zhang, A. Negi, J. He, G. Hu, S. Tian, J. Liu, Synergistic Effects of Boron Nitride (BN) Nanosheets and Silver (Ag) Nanoparticles on Thermal Conductivity and Electrical Properties of Epoxy Nanocomposites, Polym. 12 (2020).

[4] C. Ji, Y. Wang, Z. Ye, L. Tan, D. Mao, W. Zhao, X. Zeng, C. Yan, R. Sun, D.J. Kang, J. Xu, C.-P. Wong, Ice-Templated MXene/Ag–Epoxy Nanocomposites as High-Performance Thermal Management Materials, ACS Appl. Mater. Interfaces. 12 (2020) 24298–24307.

[5] L. Wang, H. Qiu, C. Liang, P. Song, Y. Han, Y. Han, J. Gu, J. Kong, D. Pan, Z. Guo, Electromagnetic interference shielding MWCNT-Fe3O4@Ag/epoxy nanocomposites with satisfactory thermal conductivity and high thermal stability, Carbon N. Y. 141 (2019) 506–514.

[6] J. Wang, C. Zhang, Z. Du, H. Li, W. Zou, Functionalization of MWCNTs with silver nanoparticles decorated polypyrrole and their application in antistatic and thermal conductive epoxy matrix nanocomposite, RSC Adv. 6 (2016) 31782–31789.

[7] Z. Wang, M. Yang, Y. Cheng, J. Liu, B. Xiao, S. Chen, J. Huang, Q. Xie, G. Wu, H. Wu, Dielectric properties and thermal conductivity of epoxy composites using

quantum-sized silver decorated core/shell structured alumina/polydopamine, Compos. Part A Appl. Sci. Manuf. 118 (2019) 302–311.

[8] C. Chen, Y. Tang, Z. Xue, Y. Xue, X. Xie, Y.-W. Mai, High-performance epoxy/silica coated silver nanowire composites as underfill material for electronic packaging, Compos. Sci. Technol. 105 (2014).

[9] Li, X. Li, Y. Zheng, L. Zhan, Q. Tian, X. Liu, New underfill material based on copper nanoparticles coated with silica for high thermally conductive and electrically insulating epoxy composites, J. Mater. Sci. 54 (2019).

[10] C. Fu, C. Yan, L. Ren, X. Zeng, G. Du, R. Sun, J.B. Xu, C.P. Wong, Improving thermal conductivity through welding boron nitride nanosheets onto silver nanowires via silver nanoparticles, Compos. Sci. Technol. 177 (2019).

[11] Y. Feng, X. Li, X. Zhao, Y. Ye, X. Zhou, H. Liu, C. Liu, X. Xie, Synergetic Improvement in Thermal Conductivity and Flame Retardancy of Epoxy/Silver Nanowires Composites by Incorporating “Branch-Like” Flame-Retardant Functionalized Graphene, ACS Appl. Mater. Interfaces. 10 (2018) 21628–21641.

[12] Kresse, G., and Furthmüller, J. (1996). Efficiency of ab-initio total energy calculations for metals and semiconductors using a plane-wave basis set. Comput. Mater. Sci. 6, 15–50.

[13] Kresse, G. (1993). *Ab-initio Molekular Dynamik für flüssige Metalle*. na.

[14] Kresse, G., and Furthmüller, J. (1996). Efficient iterative schemes for ab initiototal-energy calculations using a plane-wave basis set. Phys. Rev. B 54, 11169–11186.

[15] Kresse, G., and Joubert, D. (1999). From ultrasoft pseudopotentials to the projector

augmented-wave method. Phys. Rev. B 59, 1758–1775.

[16] Perdew, J.P., Burke, K., and Ernzerhof, M. (1996). Generalized Gradient Approximation Made Simple. Phys. Rev. Lett. 77, 3865–3868.